Impacts of selective logging on Amazon forest canopy structure and biomass with a LiDAR and photogrammetric survey sequence

d'Oliveira, Marcus Vinicio Neves; Figueiredo, Evandro Orfanó; Almeida, Danilo Roberti Alves de; Oliveira, Luis Claudio; Silva, Carlos Alberto; Nelson, Bruce Walker; Cunha, Renato Mesquita da; Papa, Daniel de Almeida; Stark, Scott C.; Valbuena, Ruben

Forest Ecology and Management

DOI:
10.1016/j.foreco.2021.119648

Published: 15/11/2021

Peer reviewed version

Impacts of selective logging on Amazon forest canopy structure and biomass with a LiDAR and photogrammetric survey sequence

Marcus Vinicio Neves d'Oliveira[1]; Evandro Orfanó Figueiredo[1]; Danilo Roberti Alves de Almeida[2]; Luis Claudio Oliveira[1]; Carlos Alberto Silva [3]; Bruce Walker Nelson[4]; Renato Mesquita da Cunha[5]; Daniel de Almeida Papa[1]; Scott C. Stark[6] and Ruben Valbuena[7]

[1] Embrapa Acre, Rodovia BR-364, km 14, CEP 69900-056 Rio Branco, Acre, Brazil; marcus.oliveira@embrapa.br; evandro.figueiredo@embrapa.br; luis.oliveira@embrapa.br; daniel.papa@embrapa.br.

[2] Department of Forest Sciences, "Luiz de Queiroz" College of Agriculture, University of São Paulo (USP/ESALQ), Piracicaba, SP, Brazil; daniloraa@usp.br

[3] School of Forest, Fisheries, and Geomatics Sciences, University of Florida, Gainesville, Florida, 32611, USA. c.silva@ufl.edu

[4] National Institute for Amazon Research (INPA), Manaus, AM, Brazil bnelsonbr@gmail.com

5 Instituto de Meio ambiente do Acre, Rio Branco, Acre, Brazil, renatomc28@gmail.com

[6] Department of Forestry, Michigan State University, East Lansing, MI, USA scottcstark@gmail.com

[7] School of Natural Sciences, Bangor University, Bangor, UK r.valbuena@bangor.ac.uk

Abstract

Sustainable forest management relies on good knowledge of forest structure obtained from ground surveys combined with remote sensing. Capable of detecting both the forest floor and canopy elements, airborne LiDAR can estimate forest structure parameters with accuracy and precision, but is still difficult to acquire due to the lake of service provider in remote regions of developing countries. Alternatively if ground surface elevations are known (e.g., from LiDAR), they can be tied to a canopy surface model derived from stereo photogrammetry using RGB images from inexpensive unmanned aerial vehicles (UAV), thus reducing the cost of post-harvest forest structure monitoring. Here we assessed whether such photogrammetric canopy measurements offer aboveground biomass (AGB) and disturbance impact estimates from logging that are comparable to LiDAR, and whether the use of both in sequence can provide an efficient post-harvest monitoring system. Specifically, through a combination of forest inventory ground plots, airborne LiDAR data, and a UAV-RGB camera system we (i) automatically located and measured canopy disturbance caused by logging, (ii) compared AGB models produced by LiDAR alone and the combination of LiDAR (for terrain elevation model) and RGB-photogrammetry (for forest surface model), and (iii) estimated the AGB stock loss from logging. The study was carried out in the Antimary State forest located in the southwestern Brazilian Amazon. Our results demonstrate that the use of RGB-photogrammetry in regions where the terrain elevation has already been estimated can be an inexpensive and effective way to rapidly identify selective logging and to accurately monitor its impact.

Key words: unmanned aerial vehicle; forest monitoring; remote sensing; digital terrain model; LiDAR; Amazon forest; carbon stocks; photogrammetry

1. Introduction

The capacity of tropical forests to be sustainably managed for timber is an important question for the conservation of biodiversity and ecosystem services such as carbon sequestration (Asner et al., 2005). Sustainable production of tropical forests, however, is questionable due to inadequate regeneration potential of valuable timber species and slow ecological recovery times (Zimmmerman & Kormos, 2012). Recent studies also provide strong evidence that rates of tree mortality are increasing in tropical forests due to climate change (Mc Dowell, et al., 2018). In the Amazon, forest carbon sinks are declining (Brienen et al., 2015), while the time required for managed forests to recover commercial timber stocks has been longer than expected (MacPherson et al., 2010; Piponiot et al., 2019), which may be linked to broad decreases in tree demographic performance. On the other hand, forest management, when practiced according to reduced impact logging prescriptions (Sist & Ferreira, 2007; Putz et al., 2008), is considered a desirable economic land use due to low carbon emissions and the conservation of forest structure, biodiversity, and environmental services (Holmes et al., 2002; Bicknell et al., 2015; Griscom et al., 2019). To evaluate the effectiveness and sustainability of tropical forest timber management reliably, cost effective and scalable approaches for forest canopy structure monitoring are critically needed.

Developing sustainable forest management depends on consistent knowledge of forest structure and species composition, traditionally obtained from ground-based surveys and forest inventories, but now increasingly relying on these surveys in combination with remote sensing tools (Prandi et al., 2016). In forest management plans this information is used to select species for logging and those for preservation, determine logging intensity, locate permanent conservation areas and, from the target tree locations and topographical information obtained from field surveys, to plan a minimal impact infrastructure layout: roads, log landings and skid trails (Figueiredo et al., 2007). Assessing the outcome of logging in terms of reduction of biomass and increase in disturbance, and monitoring forest recovery and regrowth dynamics is essential. Such assessments can ensure that forest operations were consistently executed in the field and allow monitoring of timber stocks for subsequent harvest cycles (Griscom et al., 2019). UlAccurate monitoring is essential for long-term forest production prognoses and improved understanding of tropical forest ecosystems under harvesting regimes. In addition, accurate aboveground biomass (AGB) estimates are crucial to monitoring carbon stocks to implement and verify REDD+ (Reducing Emissions from Deforestation and Forest Degradation-plus) and for broader global forest management targets and programs (Phua et al., 2016; Kronseder et al., 2012). Thus, quantifying the impact of logging on canopy structure is important to understand

the effects of forest management on forest fauna, micro-climates and regeneration processes (Pereira et al., 2002). Ground-based forest inventories, including permanent survey plots, are difficult to establish and maintain. These plots are expensive, labor intensive, and often suffer from seasonal and other access limitations specially in the tropics. Furthermore, due to low sample intensity, field plots may fail to accurately estimate forest structural parameters and their variation throughout the landscape, highlighting the need for remote sensing to better assess forest change, particularly after the impact of natural and anthropogenic disturbance events (Espirito Santo et al., 2014).

The use of LiDAR (Light Detection and Range) is well established as a remote sensing tool for estimating forest structural parameters and monitoring forest disturbance and regeneration in boreal, temperate, and tropical forests (Wulder et al., 2008). Practical and efficient, airborne LiDAR is the preeminent tool to estimate forest structural parameters related to biomass and biomass turnover (Drake et al., 2002; Asner et al., 2011; Huang et al., 2013; Palace et al., 2015; Ferraz et al., 2018; Jarron et al., 2020) and for forest monitoring and management, including assessment of logging impact (Dandois and Ellis, 2010; Réjou-Méchain et al., 2015; Silva et al., 2017; Griscom et al., 2019; Pinagé et al., 2019). However, LiDAR coverage are still difficult to hire especially in remote regions of developing countries due to the lack of established LIDAR vendors in these regions (Melendy et al., 2018, Ota et al., 2019). As an alternative, the need for LiDAR survey for forest monitoring may be reduced to a single survey, if biomass (AGB stock) resurveys can be adequately accomplished with unmanned aerial vehicles (UAV) carrying light-weight and low cost camera systems for photogrammetric structure reconstruction (Zahawi et al., 2015; Jayathunga et al., 2018).

The last decade, in particular, has witnessed an increase in the use of 3D remote sensing techniques (Valbuena et al., 2020): both passive (e.g. RGB and multispectral cameras) and active LiDAR (Almeida et al., 2019) sensors have been coupled to UAVs to perform forest surveys and assessments (Colomina and Molina, 2014). The rapid expansion of UAVs in forest research has been prompted by low acquisition and maintenance costs and ease of use. In addition, the rapid development of UAV platforms including long-distance radio control range, high-resolution RGB, multispectral cameras and automatic processing algorithms of stereo imagery facilitate the application of low-cost UAVs in the acquisition of stereo imagery (Ni et al., 2019).

The stereo imagery acquired by optical sensors onboard UAVs, photogrammetrically processed by 3D reconstruction software to generate digital terrain (DTM) and surface models (DSM) similar to those from LiDAR (Wallace et al., 2016). Moreover, while LiDAR sensors mounted on

UAVs show potential (Almeida et al., 2019; d'Oliveira et al., 2020; Prata et al., 2020), due to weight, sensor range (limiting flight height) and battery limitations only photogrammetric drones can currently survey relatively large areas (e.g. Bourgoin et al., 2020). For these reasons, 3D remote sensing from photogrammetric UAVs has become a relatively cost-effective option for measuring forest spatial structures and aboveground biomass stocks. The key limitation of this passive remote sensing approach to vegetation height estimation is the inability to identify the ground below the canopy. Active sensing in the form of LiDAR laser ranging pulses pass through the canopy to reflect off the ground surface offering statistical algorithmic approaches for terrain estimation (Axelsson, 1999). In contrast, photogrammetric surface height estimation has a very limited capacity to reach the ground for terrain estimation particularly in closed-canopy forest. For this reason, in forests, passive photogrammetric canopy height estimation is most effective when paired with preexisting accurate digital terrain modeling, for instance derived from LiDAR. To produce accurate DTMs under dense forest canopy, LiDAR is currently the most reliable approach (Crespo-Peremarch et al., 2020). Particularly when topographic variation is high, DTMs are essential to produce accurate AGB models and 3D analyses (e.g. gap fraction and height profile analyses) because the true height of the trees must be known to capture these variables related to wood and leaf mass.

To overcome combined limitations of LiDAR costs and terrain estimation, a few trail-blazing studies have combined optical and LiDAR sensors in forests in Sweden and Italy, with accurate results (Bohlin et al., 2012; Prandi et al., 2016). This approach appears particularly successful and cost-effective in studies that demand multi-temporal surveys for recovery / impact response assessment, (e.g. Mendes de Moura et al., 2019), reducing the need for an expensive LiDAR survey to only the first 'baseline' observation time point, with passive optical drone-based thereafter.

There are a considerable number of studies involving the use of LiDAR data to assess logging impact (e.g. Kronseder et al., 2012; Kent et al., 2015; Rex et al., 2020; Nunes et al., 2021), but very few have assessed selectively logged tropical forests through the combination of photogrammetry and LiDAR (e.g. Ota et al., 2019). Here, we expand this new research domain, studying the impacts of selective logging in the Antimary State Forest in the southwestern Brazilian Amazon with a photogrammetry-derived DSM and a LiDAR-derived DTM.

The aim of this paper was to verify the potential of combining a multitemporal sequence of ground data, airborne LiDAR, and 3D photogrammetry, to monitor forest disturbance after reduced-impact selective logging. Our specific objectives were to (i) estimate structural changes

in the forest canopy produced by logging operations (roads, log landings, felled tree gaps and skid trails), (ii) develop and verify the consistency of two AGB models, one produced by height metrics derived from LiDAR data alone, and the second by a combination of the LiDAR-derived DTM and a photogrammetry-derived DSM, and (iii) to upscale the developed AGB models from plot to local level to estimate the AGB stocks before and after logging, and infer subsequent AGB loss.

2. Methodology

2.1. Study Site

The Antimary State Forest (ASF) is located between Rio Branco and Sena Madureira in Acre State, Western Brazilian Amazon (68° 01' to 68°23' W; 9° 13' to 9° 31' S). The ASF covers an area of 45,490 ha (Figure 1). The climate is classified as Awi (Köppen) with an annual precipitation of around 2,000 mm and an average temperature of 25 °C. There are distinct wet and dry seasons. The dry season occurs from June to September. This season is used to prepare the land for crops and for all operations related to forest management (Carvalho et al., 2017). In the ASF there are three types of forest: dense tropical forest with uniform canopy and emergent trees; open tropical forest with frequent occurrence of lianas and palm trees; and an open forest, called Tabocal, which is dominated by semi-climbing *Guadua* bamboo species locally known as Tabocas. The area has gentle topography with a maximum elevation range of around 300 m. The predominant soils are dystrophic yellow latosols with high clay content. The ASF is administered by the Acre State Government through a forest management plan for sustainable timber production (Funtac, 1990).

The total area under forest management is 37,687 ha, divided into 14 Annual Production Units (APU) and one "absolute" forest reserve (area in the forest management plans designated for preservation only, Figure 1). In 2012, a forest concession system was adopted to regulate the execution of forest operations by logging companies, following the Modeflora methodology (Figueiredo, 2007). Our study was carried out in the APU3 (3,835 ha), which was selectively logged in 2013 and 2017. For the study, we selected an area of 42 ha logged in 2013 and another of 182 ha logged in 2017 (Figure 1C, (Figure S1 in the Supplementary Material). In both cases the logging intensity was around 10-15 $m^3 \cdot ha^{-1}$ (Carvalho et al., 2017).

In 2013, before forest logging, 10 1-ha (100 x 100 m) permanent sample plots (PSP) were established, systematically distributed in the 1,000 ha portion of the APU3 covered by airborne LiDAR (Fig. 1). Immediately after PSP establishment, the area was partially logged, affecting five

178 PSPs. After 2013, there were no additional interventions in the PSPs, which were re-measured
179 in 2015. In this paper, we used this measurement (2015) to build LiDAR and photogrammetry-
180 LiDAR AGB models. In these plots, all trees with DBH ≥ 10 cm were tagged, species identified
181 and measured. For each tree, oven-dry aboveground biomass in Mg (AGB) was estimated with
182 Eq. (1), specifically developed for the ASF (Melo, 2017).

183 $AGB = AGB = ((DBH)^{2.671} \cdot 0.064)/1000$ Eq. 1

184 Plot locations (corners) were mapped using survey-grade, dual frequency (L1 and L2), dual-
185 constellation (GPS and GLONASS) global navigation satellite system (GNSS) receivers. One-
186 second epoch GNSS data were collected for 20-30 minutes at each plot corner (d'Oliveira et al.,
187 2012). The GNSS receiver used in this study was a TechGeo Zenite II. For the GNSS field survey
188 campaign, rover receiver data were post-processed using the Rio Branco base station (RIOB
189 93911, reference station of the Brazilian Network for Continuous Monitoring – RBMC), located
190 at Acre Federal University, 90 km from the study site.

191

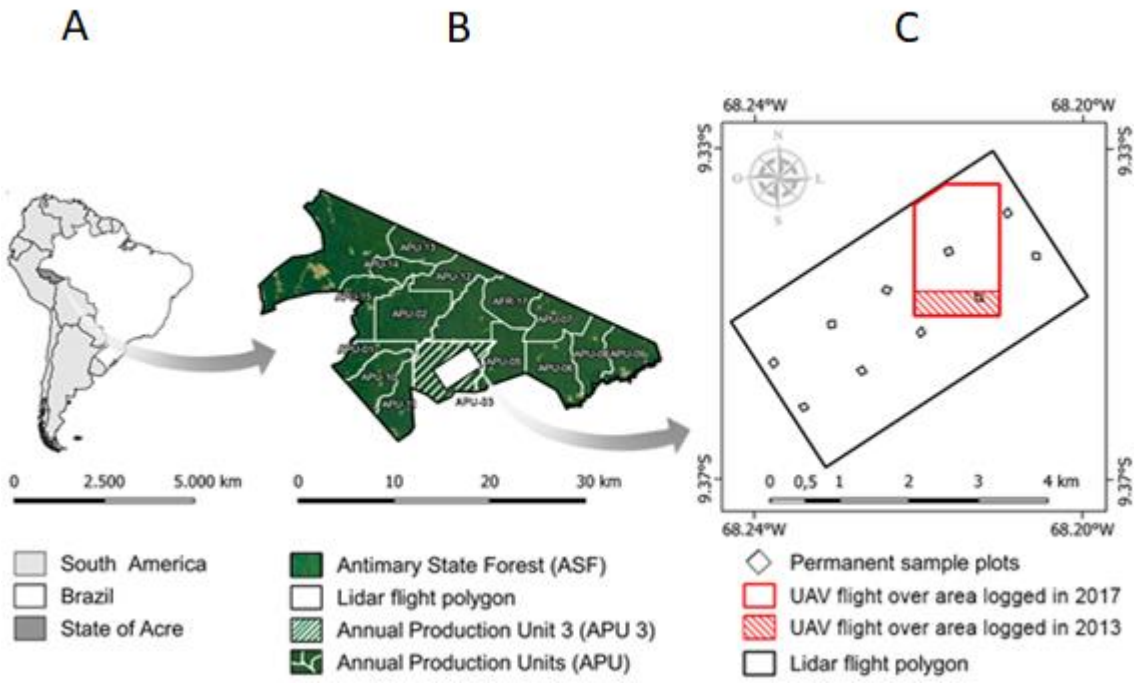

192

193 Figure 1. A. Antimary State Forest (ASF) location; B. forest management annual production units
194 (APU) and absolute forest reserve area (AFR); C. the Study area showing: (i) 1,000 ha covered by
195 LiDAR flight in 2015 (white polygon); (ii) the 182 ha area logged in 2017 (red polygon) and the
196 42 ha area logged in 2013 (red hatched polygon) covered by the UAV flight; and (iii) the
197 permanent sample plots (black squares).

198

2.2. LiDAR data acquisition and processing

Discrete return airborne LiDAR data were collected in September 2015 after UPA3 was partially logged, using a Trimble Harrier 68i sensor set to 300 kHz, installed in a Cessna 206 aircraft, flying at 600 m above ground level (AGL), with an average speed of 198 $km \cdot h^{-1}$. LiDAR sidelap was 50%, resulting in a point cloud with an average density of 14 $returns \cdot m^{-2}$ (Table S1, Figure S2 in the Supplementary Material), covering an area of 1,000 ha.

The FUSION LiDAR package (USDA Forest Service) was used for processing LiDAR data. LiDAR returns that occurred within each of the 10 PSPs were extracted from the acquisition datasets to create an all-returns point cloud file for each PSP. The ground surface elevation (interpolated from the LiDAR ground returns) was then subtracted from each return to height above ground, removing topographic variation within the plot. Descriptive statistics of the LiDAR point cloud vertical structure, using all returns above 1 m, were computed for each plot. The one-meter minimum height above ground was used to reduce noise within the near-ground point cloud caused by low vegetation and imperfections in the ground point filtering (McGaughey, 2018).

The following layers were produced at a 1 × 1 m spatial resolution: DTM, DSM, and a subsequent canopy height model (CHM = DSM - DTM), which was used to locate the forest logging operations carried out in 2013 (Figure 1). Raster layers of forest canopy metrics (Table 1) (McGaughey, 2018) were created using FUSION, following the same methodology used by d'Oliveira et al., (2012). PSP-level LiDAR metrics were merged with the summarized field plot data (collected in 2015) for regression modeling. We then created from the LiDAR point clouds, at a 100 × 100m resolution, raster layers for the forest structure metrics selected as predictor variables for the AGB models. The raster cell resolution was equal to the nominal ground plot size and the AGB model was applied over the entire 224 ha study area.

223 **Table 1.** LiDAR-and RGB point clouds derived forest structure metrics used to compose the
224 AGB models.

Metric abbreviation	Metric description
HMEAN	Mean height above ground
HMEDIAN	Median height above ground
HMODE	Mode height above ground
HSD	Standard deviation of height above ground
HVAR	Variance of height above ground
HCV	Coefficient of variation of height above ground
HIQ	Interquartile distance of height above ground
HSKEW	Skewness of height above ground
HKURT	Height kurtosis of height above ground
H. % (e.g., H05TH – H99TH)	Percentiles of height above the ground (AGL): 5th, 10th, 20th, 25th, 30th, 40th, 50th, 60th, 70th, 75th, 80th, 90^{th}, 95^{th}, 99^{th}
CCR	Canopy relief ratio (CCR = ((MEAN - MIN) / (MAX – MIN)))

225 **2.3. UAV-RGB image acquisition and processing**

226 The photogrammetric mapping was carried out in two flight campaigns. The first in September
227 2016, over the 10 PSP and the second in September 2017, covering the 182 ha (logged in 2017)
228 and 42 ha (logged in 2013), shown in Figure 1. The flights were performed with a unmanned
229 aerial vehicle (UAV), model Phantom 4 PRO. The UAV was equipped with a high-grade GNSS
230 system, barometer, accelerometer, gyroscope, compass and 20-megapixel Sony EXMOR RGB
231 camera, with a lens system of focal distance equivalent to 35 mm, coupled with a 3-axis
232 electronic gimbal. Flights were performed autonomously, with a constant speed of 12 $m \cdot sec^{-1}$,
233 160 m above the ground and 80% frontal and lateral overlap. The ground sample distance (GSD)
234 was 4.39 cm and the point cloud average returns density was 112.5 m^{-2} (Figure 2).

235 We used the structure from motion (SfM) process to generate point clouds. The RGB images
236 were mosaicked and orthorectified with Pix4D Mapper software through the SIFT (Scale-
237 Invariant Feature Transform) procedure (Table S2, Lowe, 2004). The products generated were
238 an orthophoto mosaic, and a digital surface model (DSM) for both the ground plots and the areas
239 logged in 2013 and 2017.

240 As LiDAR and UAV systems data are similar in nature and geographically coincident, rasters
241 produced by photogrammetry (orthomosaic and digital terrain and surface models) were
242 automatically aligned to the LiDAR products (LiDAR – UAV products geolocation RMSE < 0,3m,
243 ESRI, 2006; Liu, 2013; d'Oliveira et al., 2020). As previously noted, DTMs produced by passive
244 sensors over dense forest canopy are not accurate (Ni et al., 2019). Thus, to produce the UAV
245 system Canopy Height Model (CHM), we used the LiDAR DTM as ground reference. This
246 approach has been regularly used in similar studies (Bohlin et al., 2012; Jayathunga et al., 2019),

by simply subtracting the LiDAR-DTM elevation from the UAV-DSM. The vegetation metrics were extracted following the same methodology applied to the LiDAR data.

2.5. Logging gaps and canopy cover loss

The detection of areas damaged by logging was carried by three methods: (i) post-disturbance automatic gap detection, (ii) manual vectorization of visually detected disturbance and infrastructure features and (iii) automatic detection of the removed crowns taller than 30m. Automatic gap detection was by a time-static analysis of the post-disturbance CHM derived from the UAV point cloud normalized to the LiDAR DTM.

To the automatic gap detection (method i), we adapted a gap definition similar to Brokaw (1989), in which, in a classical sense, gaps are openings in the forest canopy extending down to an average height ≤ 2 m aboveground adapted from Asner et al. (2013). Thus, logging gaps were defined by a low height threshold (CHM < 3 m) and by a minimum 20 m2 area, to exclude small gaps that were more likely produced by natural causes. The 3m threshold was used to allow the inclusion of the felled trees crowns on the ground as gaps.

We quantified the visual vectorization of disturbances in the entire area covered by UAV flights and compared results to method (i). The vectorization was performed using the high-resolution RGB orthophoto mosaic to identify all logging operation features (roads, landings, felled tree gaps and skid trails). The overlapping area of agreement between the two methods was found by the spatial intersection of their respective logging damage polygons.

We assessed felling of tall trees, whether logged or from ancillary damage. To quantify disturbance, we subtracted pre- and post-logging CHM, but only for points above 30 m height (adapted from Andersen, et al., 2014). To avoid including small gaps produced by natural causes (e.g. broken branches, inter-crown spaces, differences in UAV and LiDAR system crown delineations), we used a minimum crown projection area patch (CPA) of 100 m^2 (Figueiredo et al., 2016). The number of felled tall trees was estimated by counting the resulting “lost tree crown” polygons. All polygons were visually validated in the 2017 orthomosaic to confirm the CPA loss.

2.6. LiDAR and UAV systems data regression modeling of aboveground biomass

Multiple linear regression was used to develop relationships between plot-level metrics derived from LiDAR and UAV point clouds, and the field measured AGB of the same plots. This was done for the 2015 LiDAR-only point cloud and the 2016 UAV hybrid point clouds that were normalized

to LiDAR DTM. Predictor variables (Table 1) from both the LiDAR and the UAV-hybrid point clouds were selected, using the best-subsets approach. Variance inflation factor (VIF) statistics were used to eliminate highly collinear predictor variables (Fox & Monette, 1992). If VIF exceeded 5.0 for a candidate predictor variable, it was dropped from the regression model.

To contrast AGB estimates from LiDAR and UAV systems , we estimated AGB across the 224 ha area covered by LiDAR in 2015 before logging and by UAV in 2017 after logging, at 100 × 100 m resolution (Dandois and Ellis, 2013; Jayathunga et al., 2018; Ota et al., 2019). To avoid the differences in AGB stocks produced by selective logging in the studied area, the consistency of the produced models was tested only in the area logged before the LiDAR flight in 2015 (42 ha area, Figure 1). An estimate of the AGB loss was performed by the subtraction of the AGB stocks estimated by the models before (LiDAR-System) and after (UAV-System) logging.

Results

3.1. Canopy disturbed by logging areas

Gaps of less than 3m height and larger than 20m^2 were infrequent in the study site before logging, with most located in the southern portion, which was logged in 2013 (Figure 2). Areas disturbed by logging in 2017 (roads, landings, skid trails and felled tree gaps) were easily distinguishable in the high-resolution September 2017 UAV orthomosaic (Figure 3A and 3). The hybrid CHM height break of 3 m effectively identified the gaps produced by logging operations (Figure 4C). The total gap area detectably produced by logging operations on the ground was calculated as 15.5 ha out of the total 182 ha covered by the UAV flights performed immediately after logging in 2017 (Table 2). This area represents 8.5 % of the mapped logged area. The logging damage manual vectorization (Figure 3C) identified a total logging impact of 17.4 ha, distributed in roads (5.5 ha), log landings (1.2 ha) and felled tree gaps and skid trails (10.7 ha). Skid trails and felled tree gaps were classified together, due to the difficulty in separating them close to tree gaps and in properly identifying skid trail fragments covered by the forest understory. Differences observed in roads and felled tree gaps were mainly promoted by automatic detection underestimation of road areas due to tree crown projections over the roads and the overestimation of the felled tree gaps by visual detection. Outside the intersection area, automatic detection was able to identify logging gaps, skid trails and roads and landings that had been partially missed by manual vectorization. Some natural gaps, low vegetation areas and deciduous trees were also automatically detected as logging damage gaps (Table 2).

Gap area determined by manual vectorization in general produced gaps that encompassed larger border areas, included standing trees and residual vegetation inside the gap as part of the impacted area (Figure 4); furthermore, this vectorization connected a second gap not clearly associated with the felled tree that was not found by automatic gap detection. The logging-impacted area that was automatically detected produced two gaps, separated by residual vegetation: a small area located on the left branch (black triangle over the felled tree crown) extrapolated the elevation difference between DSM and DTM that had been established for logging impact classification (3 m) and was classified as non-logged area. The differences observed in this figure summarize the main differences observed between the two methods.

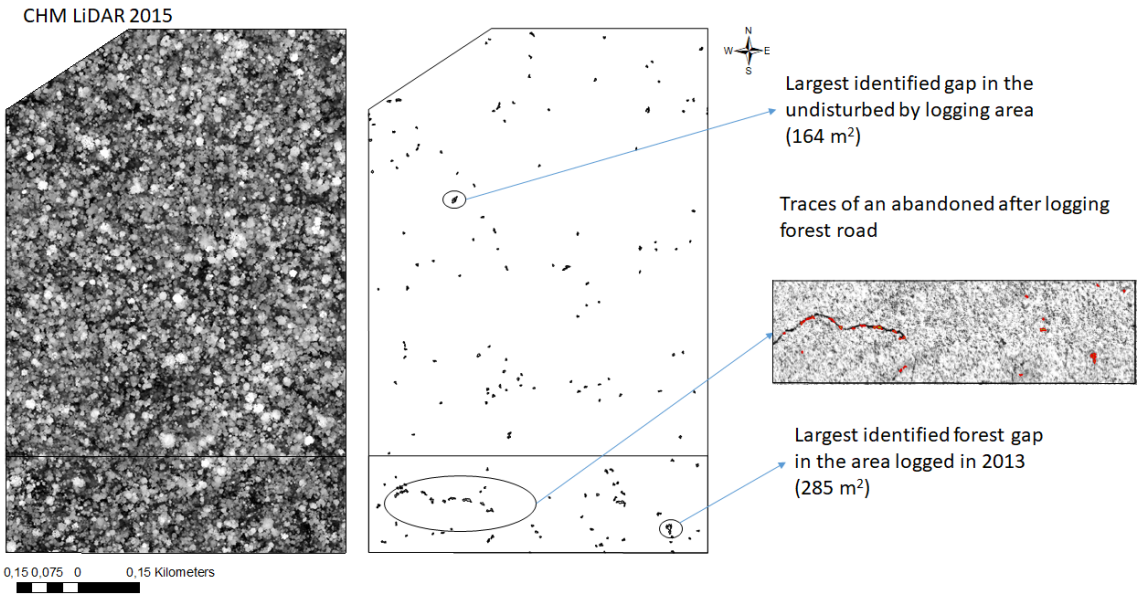

Figure 2. Canopy height model and logging gaps (CHM < 3 m, area > 20 m^2) before 2017 logging (LiDAR flight in 2015). In the south part of the study area, it is possible to observe traces (roads and tree felling gaps) from the logging carried out in 2013.

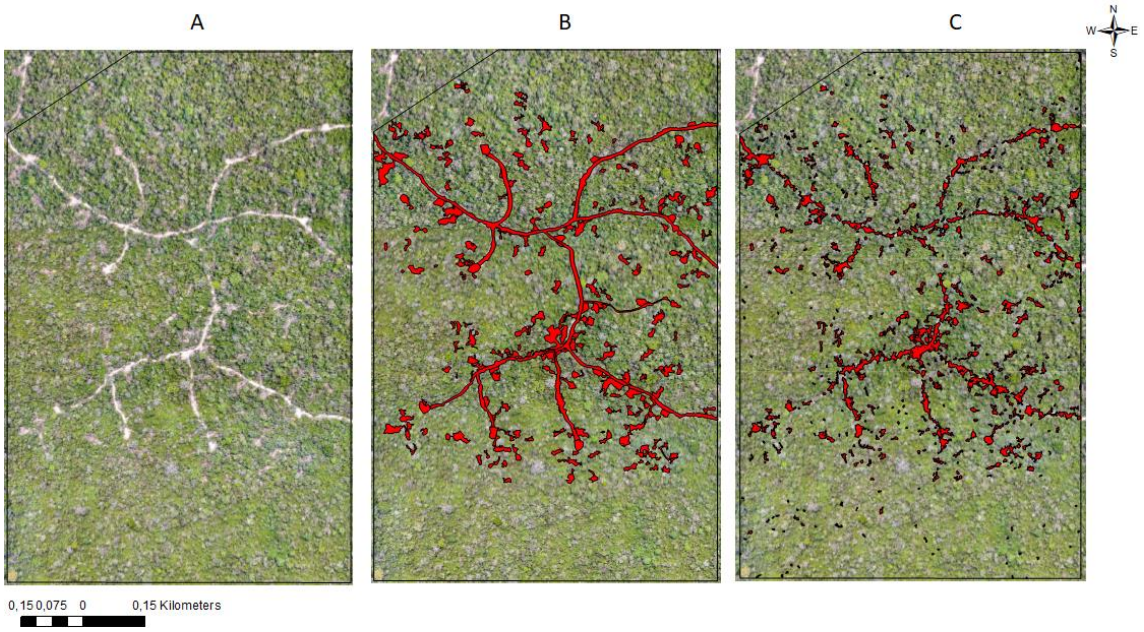

Figure 3. Area covered by the UAV flight (224 ha) in 2017 immediately after logging, presenting: A. The high-resolution (4 cm) orthomosaic; B. The orthomosaic with the areas automatically identified as disturbed by logging (DSM ≈ DTM, area ≥ 20 m^2) and C. The manual vectorization of roads, landings and felled tree gaps.

Table 2. Areas impacted by logging (ha) automatically identified and manually vectorized in the UAV flight of area logged in 2017 (182.9 ha). The areas identified as 'other' are natural gaps, low vegetation and deciduous trees.

Method	Roads (ha)	Logs landing (ha)	Felled tree gaps and skid trails (ha)	Other (ha)	Total (ha)
Vectorization	5.5	1.2	10.7		17.4
Automatic detection	4.4	1.1	9.6	0.5	15.5
Intersection	3.4	1.1	6.1		10.1

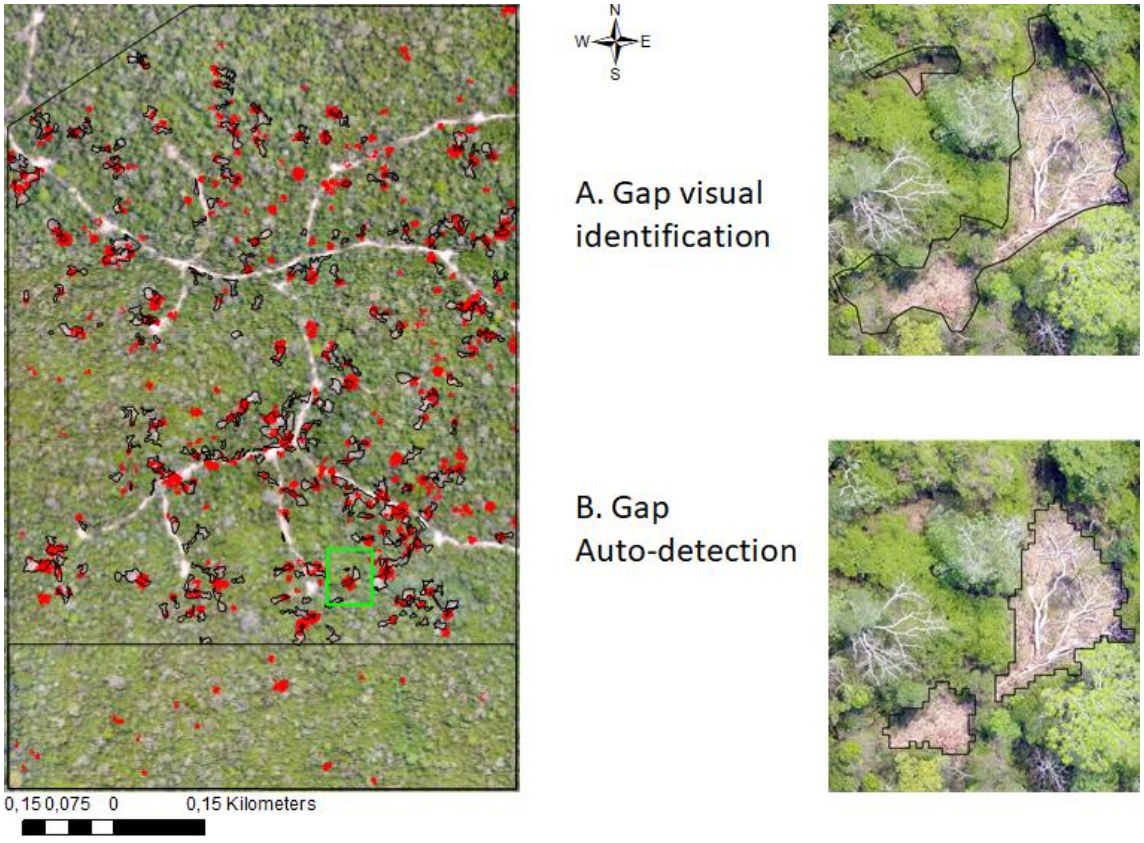

Figure 4. Felled tree gaps determination by A. visual interpretation and B. automatic detection (CHM ≤ 3 m, gap area ≥ 20 m^2) in a felled tree gap. Highlighted green square represents zoomed-in tree fall gap. In the orthomosaic red polygons represent the removed tree crowns and the black ones the automatically detected felled tree gaps.

The canopy cover area above 30m height (minimum CPA 100 m^2) was 47.7 ha before (Figure 5A) and 31.0 ha after logging (Figure 6B). The estimated tall tree crown canopy loss produced by logging was 11.3 ha (307 trees) or 23.7% of the original canopy cover (Figure 5B). A considerable number (134) of deciduous trees were misclassified as removed trees, representing a canopy cover of 2.4 ha. These trees were not computed as logging impact and were classified as part of the post-disturbance standing crown projection area (Figure 5C and D). Small gaps, broken branches, small tree crowns (CPA < 100m2), inter-crown spaces, differences in UAV and LiDAR

system crown delineations, resulted in an canopy area of 5.4 ha. The applied method to canopy cover loss automatic detection allowed the identification of individual logged trees crowns (Figure 7). The automatic detection of canopy cover loss allowed the identification of individual logged trees crowns (Figure 6).

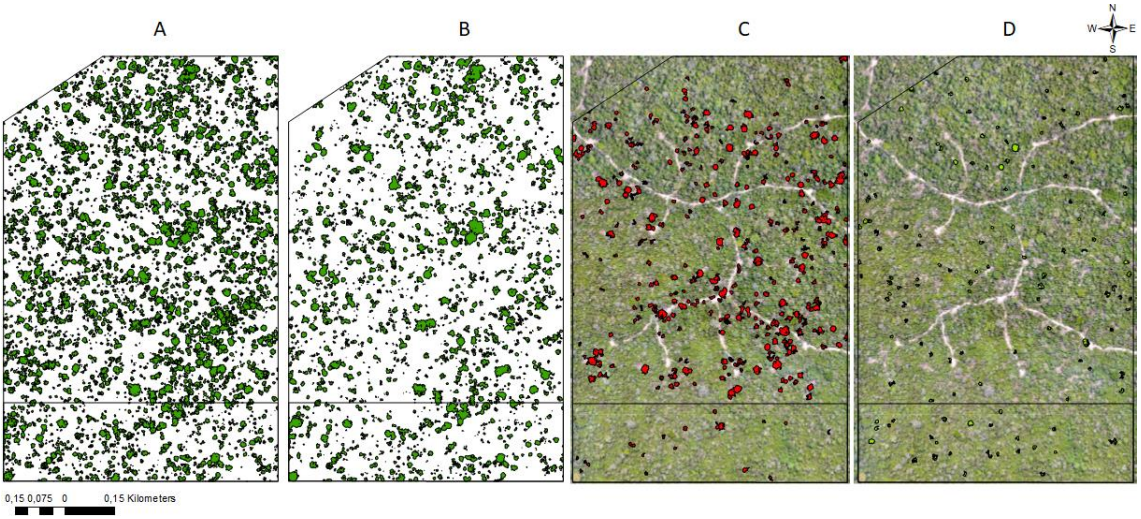

Figure 5. Canopy cover above 30 m (crown projection area patch ≥ 100 m^2): A. Before logging (2015 – 47.7 ha); B. After Logging (2017 – 31.0 ha); C. Canopy cover loss (11.0 ha) and D misclassified deciduous trees (2.4 ha). Green polygons (A, B and C) represent alive tree crowns and red polygons (D) removed tree crowns.

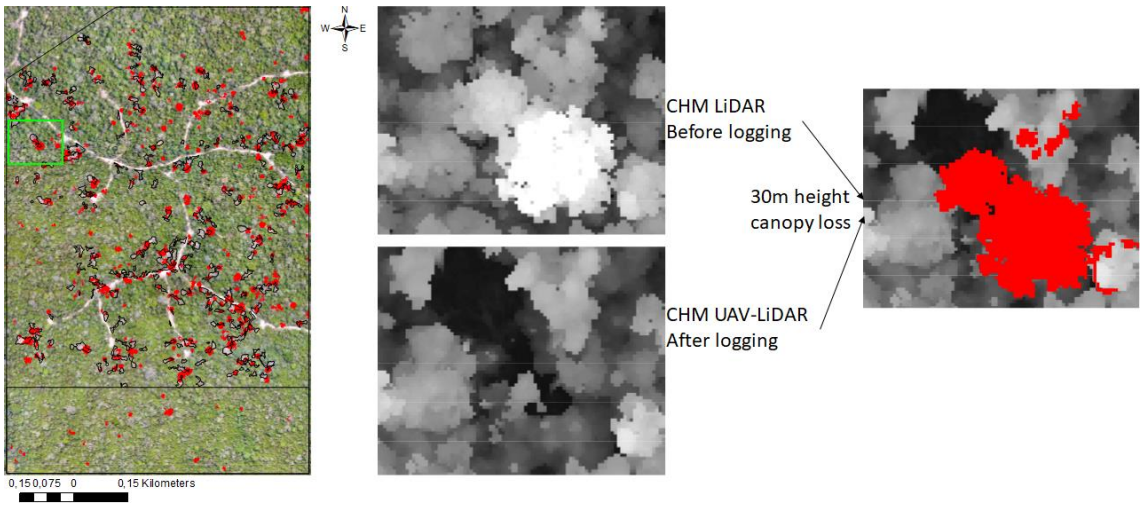

Figure 6. Zoomed tree fall gap presenting: i. the CHM LiDAR before logging (2015); ii. CHM UAV-LiDAR (hybrid) after logging (2017) and iii. the automatically detected tall canopy cover loss (CHM ≥ 30 m and CPA ≥ 100 m^2.In the orthomosaic red polygons represent the removed tree crowns and the black ones the automatically detected felled tree gaps.

3.2. LiDAR and photogrammetry metrics-derived AGB models

The mean tree density and AGB in the plots were 346 ± 16 trees·ha^{-1} and 239.9 ± 25.4 Mg·ha^{-1} respectively (Table 4). From the point cloud metrics, two parsimonious aboveground biomass (AGB) regression models were developed. A single predictor metric was selected, 95th percentile of point heights, for both LiDAR and UAV derived point clouds. The explained variances of UAV and LiDAR models were respectively R^2 = 0.74 (residual standard error RSE = 42.8 Mg·ha^{-1}) and R^2 = 0.57 (RSE = 56.0 Mg·ha^{-1}) (Figure 7). The mean AGB estimates by the airborne LiDAR and UAV systems were 240.0 ± 21.9 Mg·. ha^{-1} and 239.8 ± 19.7 Mg·ha^{-1}, respectively.

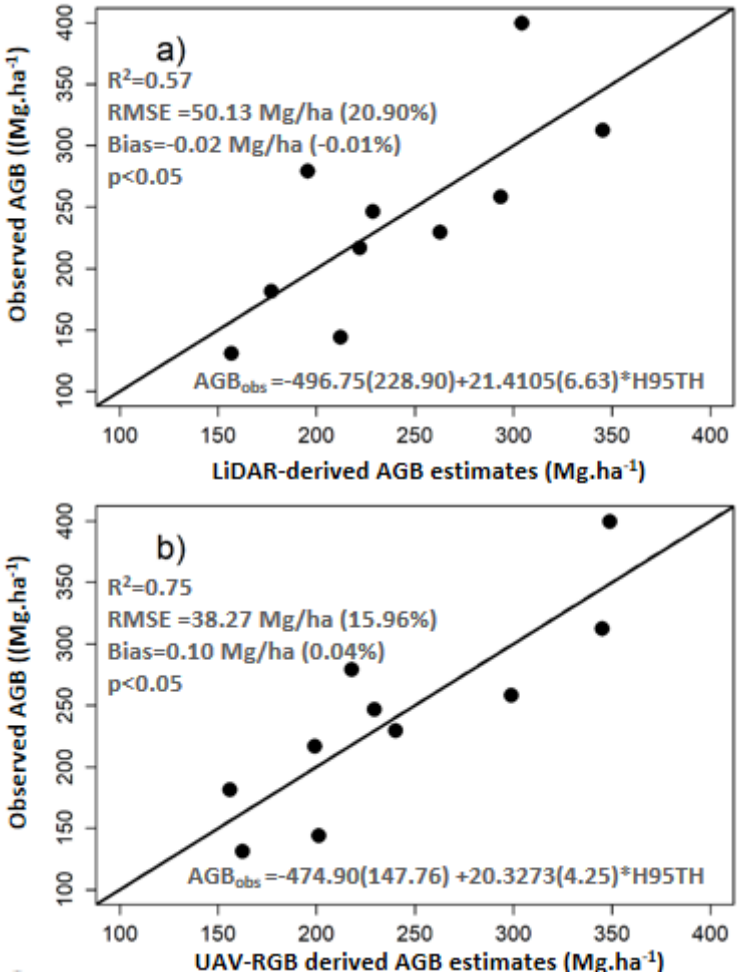

Figure 7. Predicted versus observed (ground plot) values for aboveground biomass (AGB - Mg. ha-1), for models produced by the (A) LiDAR system and (B) UAV system. Numbers in parentheses are the standard errors for each coefficient.

3.3. Landscape analyses

The mean AGB estimated for the 182 ha area logged in 2017 was 251.9 ± 55.8 Mg·ha^{-1} before logging (LiDAR system AGB model) and 226.4 ± 73.7 Mg·ha^{-1} after logging (UAV system AGB model). The lower mean AGB estimated by the UAV model is the expected AGB loss (25.5 Mg·ha^{-1}), produced by logging (Figure 8A and B). Considering only the area logged in 2013 (south part of the studied area - 42.0 ha), the AGB estimates were 213.3 ± 63.7 Mg·ha^{-1} (LiDAR) and 213.4 ± 63.9 Mg·ha^{-1} (UAV). The correlation between the UAV and LiDAR AGB models in this area was highly significant (R^2 = 0.93, SE = 17.3, p < 0,001, N = 48, Figure S3 in the Supplementary Material), attesting to the compatibility of the models.

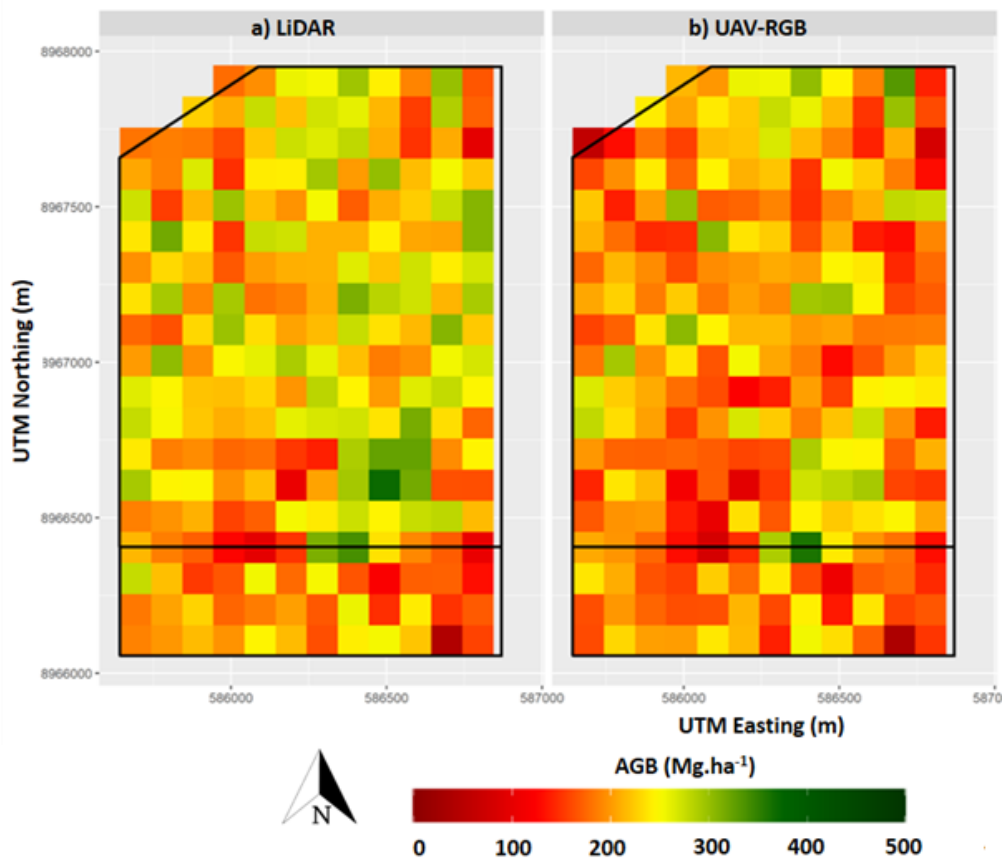

Figure 8. Aboveground biomass (AGB; Mg·ha^{-1}) estimates from the (A) airborne LiDAR and (B) UAV RGB camera systems' predictive equations, at a 100 x 100 m resolution. The area covered by the UAV is divided into two polygons: the top polygon is the area logged in 2017 (182 ha) and the bottom red polygon (42.0 ha) logged in 2013.

4. Discussion

Our analysis clearly demonstrated that photogrammetric UAV-based canopy structural estimation can be used to develop cost-effective time series of canopy structural impacts and recovery of logging in tropical forest. The essential requirement for this method is a high accuracy terrain model, which is not available from photogrammetry alone in closed canopy forest. In addition, the fusion of LiDAR and RGB-photogrammetry produced a reliable AGB model similar to the one produced by LiDAR alone. Specifically, our analyses found that (i) the area directly and heavily impacted by logging operations was 8.2% of the total study area, (ii) the tree cutting produced a canopy cover (above 30m) loss of 22.7% and (iii) selective logging produced a mean AGB loss of 27.8 Mg·ha-1.

4.1. Canopy disturbed by logging areas

Besides estimates of forest structural parameters, LiDAR data is also recognized as a key tool in identifying past logging impacts on the forest understory (Kent et al., 2015; Ellis et al., 2016; Griscon et al., 2019). In this study, we could observe traces from the 2013 logging in the southern part of the study area in both LiDAR and UAV systems flights. The traces identified by LiDAR through gap analyses were similar to those observed in a previous study with the use of a relative vegetation density (RDM) model (Pantoja, 2017) in the same site. RDM is calculated through an algorithm used to create raster layers of a relative percentage of LiDAR returns within a user-specified above ground height stratum (d'Oliveira et al., 2012). While we should expect correspondence since the studies differed in methodologies but not data sources, that these logging impacts were still possible to detect four years after logging by the UAV system reveals the great potential of this approach for forest management monitoring. We found no other study in the literature that specifically demonstrated that UAV based photogrammetry combined with pre-existing LiDAR could identify canopy loss in selectively logged tropical forests. The three-meter height break and minimum contiguous area of 20 m^2 adopted in our study, allowed the detection of all landings, logs and felled tree crowns on the ground visually identified. In a similar study (Pinagé et al., 2019), the authors used a greater (10 m) height break and a smaller area (10 m^2) to define gaps. In our case, as the UAV-system flight was carried out immediately after logging, vegetation higher than 3m as well as smaller than 20m^2 would be more likely to belong to a natural gap than a logging gap. In addition, the use of a higher threshold in a forest with moderate to high occurrence of *Guadua* spp, which often does not reach 10m, all patches of dense *Guadua* spp would be classified as gaps. The result we obtained by using of a hybrid (LiDAR + photogrammetry) CHM to determine impact in logging areas was

similar to that obtained by the LiDAR-derived relative vegetation density model (RDM) used by Carvalho et al (2017) in the Antimary State Forest, where areas impacted by logging were estimated as 7 to 8.6 % of the total managed area, but below the 15.4 % and 17.1 % estimated by d'Oliveira et. (2012) and Andersen et al. (2014), respectively. Although it was limited by the passive nature of the sensor, the method was sufficient to identify the visible disturbed areas. Similar methodology applied to photogrammetric products was used to identify the soil displacement produced by logging in a clear cutting harvesting in a temperate forest in Norway (Pierzchała et al., 2014).

Disturbed areas covered by tree crowns could not be properly classified by the hybrid photogrammetric automatic detection, producing an underestimation of the overall logged area assessment. The logging impact assessed by both methods was relatively low and can be seen as a consequence of the low harvesting rate applied in APU3, which was the result of the utilization of reduced impact logging (RIL) practices. Although the automatic detection and the visual vectorization methods presented similar areas, their locations presented some differences, due to the nature of the UAV sensor and the human error associated with vectorization. Large areas disturbed by logging were easily detected by both methods, but areas covered by vegetation, such as skid trails, were difficult to detect, leading to likely inaccuracies. Skid trails are difficult to identify even through the use of LiDAR because the drivers of logging vehicles naturally avoid felling trees (Araujo et al., 2013). In the case of our study, the main source of divergence between visual and automatic identification methods was the determination of the roads under tree crowns, which could not be identified by automatic detection. On the other hand, the visual vectorization of road borders and standing trees inside the gaps would not only be tedious and labor-intensive, but would also involve interpretation errors and impose limits on its accuracy.

Canopy loss above 30 m was much higher than that observed by Andersen et al (2014) in an adjacent annual production unit in the ASF, and by Pereira et al (2002) when RIL techniques were applied. In the Andersen et al (2014) work, using repeated LiDAR flights, the canopy cover loss above 30 m was only 4.1%. Although high, the estimated canopy loss in this study seems to be accurate. The two potential sources of error, deciduous trees and canopy cover fragments (CPA < 100 m^2), were not computed as canopy loss. Deciduous trees produced a small effect on the impacted area classification. Although the ASF presented a considerable number of leafless trees, most of them could be properly identified as different from logging gaps because the understory vegetation below them usually exceeded the 3 m height threshold for defining a gap,

but it was an issue for the extracted trees identification. Deciduous trees interfere with the 3D photogrammetric analyses (e.g. Ni et al., 2019) and, to some extent, also for LiDAR (i.e., by reducing the number of returns of big leafless crowns). However, while LiDAR can fly in both leafless and leafy seasons, allowing a possible solution in avoiding periods with the most leaf off deciduous crowns, this is not available for the UAV method. This is because the leafy season coincides with the rainy season, during which UAV flights and access to tropical forest study areas are limited, as is the case with our site.

Although we recognize that the used UAV-System has flight limitations, UAV use to forest monitoring must consider that even when we use LiDAR to monitor logging we do not cover the entire area but rather cover sampling areas large enough to represent the different treatments (dates in the case of this study). Furthermore, there is greatly increasing interest in how forests impacted by disturbances like logging may be further impacted by increasing droughts, surface fires, and other disturbances on the rise due to human impacts since interactions between disturbances can promote destructive forest loss tipping points (Bourgoin, et al., 2020; Stark et al 2020).

4.2. LiDAR and UAV system AGB models

The AGB model developed from LiDAR data estimated the ASF UPA3 mean AGB stock before logging as 231.3 $Mg \cdot ha^{-1}$. This value is almost the same as that obtained by d'Oliveira et al. (2012, 232 $Mg \cdot ha^{-1}$) in an adjacent APU in the ASF logged in 2010-1011. This was expected, because the areas are only 8 km apart and have a similar forest structure, but emphasizes LiDAR data consistency in relation to tropical forest AGB estimates. The R^2 (0.57) and RMSE (52.05-23.2 %) were also similar to values in other tropical forests in Borneo (Phua et al., 2016; Kronseder et al., 2012), Eastern Brazilian Amazon (Mendes de Moura et al., 2019; Rex et al., 2020), and Sierra Leone (Kent et al., 2015), all of which, confirm, once more, the accuracy of LiDAR data to estimate forest structural parameters.

Although the use of models produced by stereo photogrammetry are becoming common to estimate AGB in forest areas, the use of this method use in dense closed-canopy forest, is still limited by the need of ground position and elevation measurements to build an accurate high resolution DTM (Dandois and Ellis, 2010; Bohlin et al., 2012). Passive sensors only identify these ground references when gaps of sufficient size are present and afford sufficient illumination for oblique angle views needed in positional triangulation (Swinfield et al., 2019). Digital earth

models derived from space-based altimetry data are globally available, but they still offer limited canopy height accuracy in forest areas (e.g. SRTM, Farr et al., 2007). Attempts to globally correct an SRTM derived DEM have been made using LiDAR data as reference, but the uneven distribution or absence of LiDAR cover (e.g. over rain forests) decreases the accuracy of the model (Zhao et al., 2018). Thus, the use of image-based point clouds to produce AGB models in dense forests demands the availability of a high spatial resolution and vertical accuracy LiDAR DTM (White et al., 2013; Ota et al., 2015; Salach et al., 2018). One exception is the work of Ota et al. (2019) in Myanmar, who also did not use a DTM. Their vegetation metrics were obtained by subtraction from the DSM elevations derived from the photogrammetric point cloud to estimate AGB changes produced by selective logging at a 0.25ha scale. The accuracy obtained by them (R2 = 0.77 and RMSE = 9.32) was close to the obtained by our UAV-LiDAR AGB model. They also used normalized green-red bands before and after logging to estimate AGB changes at a 0.25ha scale. Furthermore, we point out that the UAV-system can capture only the upper canopy surface, which may be a problem when assessing dense forest canopy.

The point clouds generated by the UAV and LiDAR systems were characterized by two main differences, in return density, and in canopy penetration. The denser point cloud of the UAV system allows a better delineation of the crowns and the creation of a high-resolution orthomosaic (Dandois and Ellis, 2010). On the other hand, the higher canopy penetration provided by the LiDAR system allowed a much better vertical forest structure description (van Leewen & Nieuwenhuis, 2010). Despite these differences, both AGB models developed in this work selected the same top canopy metric as the best predictor variable (H95TH). Relevant to expanding UAV system photogrammetric research, Meyer et al. (2018), demonstrated that the relationship between a new LiDAR-derived index LCA (Large Canopy Trees) and AGB was linear and remained unique across forest types (R^2 = 0.78, RMSE = 46.02 $Mg \cdot ha^{-1}$). The LCA method is based on the most exposed tree crowns, hence UAV system AGB models may be a good complement since these trees are well represented by photogrammetry point clouds (White et al., 2015). The UAV model's accuracy was similar to that in other studies as well as the correlation of LiDAR vs UAV models (Dandois et al., 2010; Jensen and Mathews, 2015; Ni et al., 2019; González-Jaramillo et al., 2019). We believe that the statistical correspondence between models would be higher with flights carried out in a shorter interval, but the agreement between the models (R^2=0.93 and RMSE=17.19) was similar to that produced by d'Oliveira et al. (2020) using two LiDAR systems, a regular airborne system (similar to the one used in this study) and an UAV-LiDAR system in similar conditions. Considering the different nature of the RGB camera and LiDAR, the results obtained when comparing the AGB models produced are a strong

indicator of the photogrammetry-LiDAR hybrid model's accuracy. Silva et al. (2017) demonstrated that acceptable AGB estimation can be achieved with low-pulse-density LiDAR surveys if a high-quality DTM is available from at least one LiDAR survey. In our study, we demonstrate that, when a high quality DTM is available, it can be achieved from a UAV-RGB system.

4.3. Local analysis

The upscaling of the AGB models from plot to landscape level, to produce an AGB map for the study area, is the typical way to assess AGB stocks and AGB changes. This procedure, oftening employing data sources at multiple scales including from orbital platforms, has been applied to produce high resolution AGB maps from focal areas of particular interest (e.g. Bispo et al., 2020), to regional scales (Longo et al., 2016), or even country and global scales (Asner et al., 2013b; Saatchi, 2017). Since LiDAR data were available for the area selected to this study area, it was possible to map LiDAR estimates of AGB at 100 m resolution, which, along with the CHM, provides forest planners with more spatially accurate and detailed planning information than is possible via ground data collection methods (d'Oliveira et al., 2012). We also upscaled our models to the entire study area to assess AGB loss produced by logging. AGB LiDAR models can be generalized (Asner et al., 2011) or applied in different regions (Drake et al., 2002). In our extrapolation, AGB maps produced by both LiDAR and photogrammetric-LiDAR DTM hybrid models were highly correlated. Although the models were produced by two different sensors, in the areas not disturbed by logging the mean AGB values that we estimated were very similar and the models effectively estimated the original and remaining biomass stock, as well as the AGB loss produced by logging.

5. Conclusions

The results of our study are of practical use to scientists, forest managers and technicians from governmental environmental control agencies; the UAV system was accurate when compared with repeated LiDAR flights over the same area. The use of LiDAR to monitor AGB change under selective logging practices in the Brazilian Amazon is becoming frequent, especially in public forests. In our study, we track the location of forest logging operation impacts and changes in AGB stocks after logging. These parameters can be used to assess the quality of forest practices and monitor forest recovery, and are strong indicators of forest management sustainability.

Acknowledgements

We thank Acre State government, IADB, and CNPq for their support for establishing inventory plots and aircraft for the LiDAR flight. We thank the Embrapa Acre parabotanic team for their support during fieldwork. We thank Renata C.F. Seabra from Embrapa Acre for the bibliography review and adjustments. Finally, we thank the Fototerra team for the 2015 LiDAR vertical datum adjustment. D. Almeida was supported by the São Paulo Research Foundation (#2018/21338-3). S.C.S. is supported by the USDA NIFA and National Science Foundation (NSF) awards DEB-1950080 and 1754357.

6. Bibliography

Almeida, D.R.A., Broadbent, E.N., Zambrano, A.M.A. et al., 2019. Monitoring the structure of forest restoration plantations with a drone-Lidar system. Int. J. Appl. Earth Obs. Geoinf. 79, 192-198. https://doi.org/10.1016/j.jag.2019.03.014.

Andersen, H.E., Reutebuch, S.E., McGaughey, R.J. et al., 2014. Monitoring selective logging in Western Amazonia with repeat LIDAR flights. Remote Sens. Environ. 151, 157-165. https://doi.org/10.1016/j.rse.2013.08.049.

Araujo, L.S., Keller, M., d'Oliveira, M.V.N. et al., 2013. Dados LiDAR e análise orientada a objeto no monitoramento de manejo florestal. Artigo apresentado no XVI Simpósio Brasileiro de Sensoriamento Remoto (SBSR), Foz do Iguaçu, April 13-18.

Asner, G.P., Knapp, D.E., Broadbent, E.N. et al., 2005. Selective logging in the Brazilian Amazon. Science 310 (5747), 480-482. https://doi.org/10.1126/science.1118051.

Asner, G.P., Mascaro, J., Muller-Landau, H.C. et al., 2011. A Universal airborne LiDAR approach for tropical forest carbon mapping. Oecology 168, 1147–1160. https://doi.org/10.1007/s00442-011-2165-z.

Asner GP, Kellner JR, Kennedy-Bowdoin T, Knapp DE, Anderson C, et al., 2013. Forest Canopy Gap Distributions in the Southern Peruvian Amazon. PLoSONE 8(4): e60875. doi:10.1371/journal.pone.0060875

Asner, G.P., Mascaro, J., Anderson, C., et al., 2013. High-fidelity national carbon mapping for resource management and REDD+. Carbon Balance Manag. 8, 7. https://doi.org/10.1186/1750-0680-8-7.

Axelsson, P., 1999. Processing of laser scanner data — algorithms and applications. ISPRS J. Photogramm. Remote Sens. 54 (2-3), 138-147. https://doi.org/10.1016/S0924-2716(99)00008-8.

Bicknell, J.E.; Struebig, M.J.; Davies, Z.G., 2015. Reconciling timber extraction with biodiversity conservation in tropical forests using reduced-impact logging. Journal of applied ecology, doi: https://10.1111/1365-2664.12391.

Bispo, P.C., Rodríguez-Veiga, P., Zimbres, B. et al., 2020. Woody aboveground biomass mapping of the Brazilian Savanna with a multi-sensor and machine learning approach. Remote Sens. 12, 2685. https://doi.org/10.3390/rs12172685.

588 Bohlin, J., Wallerman, J., Fransson, J.E.S., 2012. Forest variable estimation using
589 photogrammetric matching of digital aerial images in combination with a high-resolution DEM.
590 Scand. J. For. Res. 27 (7), 692–699. https://doi.org/10.1080/02827581.2012.686625.

591 Bourgoin, C.; Betbeder, J.; Couteron, P. et al, 2020. UAV-based canopy textures assess changes
592 in forest structure from longterm degradation. Ecological indicators,
593 https://doi.org/10.1016/j.ecolind.2020.106386.

594 Brienen, R.J.W.; Phillips, O.L.; Feldpausch, T.R.; et al., 2015. Long-term decline of the Amazon
595 carbon sink. Nature 519: 344-348. https://doi:10.1038/nature14283.

596 Brokaw NV, Scheiner SM (1989) Species composition in gaps and structure of a tropical forest.
597 Ecology 70: 538–541.

598 Carvalho, A.L., d'Oliveira, M.V.N., Oliveira, L.C. et al., 2017. Natural regeneration of trees in
599 selectively logged forest in Western Amazonia. For. Ecol. Manag.392, 36-44.
600 https://doi.org/10.1016/j.foreco.2017.02.049.

601 Colomina, I., Molina, P., 2014. Unmanned aerial systems for photogrammetry and remote
602 sensing: a review. ISPRS J. Photogramm. Remote Sens. 92, 79–97.
603 https://doi.org/10.1016/j.isprsjprs.2014.02.013.

604 Crespo-Peremarch, P., Torralba, J., Carbonell-Rivera, J.P. et al., 2020. Comparing the generation
605 of DTM in a forest ecosystem using TLS, ALS and UAV-DAP, and different software tools. Int.
606 Arch. Photogramm. Remote Sens. Spatial Inf. Sci. 43, 575-582. https://doi.org/10.5194/isprs-
607 archives-XLIII-B3-2020-575-2020.

608 Dandois, J.P., Ellis, E.C., 2010. Remote sensing of vegetation structure using computer vision.
609 Remote Sens. 2 (4), 1157-1176. https://doi.org/10.3390/rs2041157.

610 Dandois, J.P., Ellis, E.C., 2013. High spatial resolution three-dimensional mapping of vegetation
611 spectral dynamics using computer vision. Remote Sensing of Environment 136, 259–276.
612 https://doi.org/10.1016/j.rse.2013.04.005.

613 d'Oliveira, M.V.N., Reutebuch, S.E., McGaughey, R.J. et al., 2012. Estimating forest biomass and
614 identifying low-intensity logging areas using airborne scanning LiDAR in Antimary State Forest,
615 Acre State, Western Brazilian Amazon. Remote Sensing of Environment 124, 479-491.
616 https://doi.org/10.1016/j.rse.2012.05.014.

617 d'Oliveira, M.V. N., Broadbent, E.N., Oliveira, L.C.et al., 2020. Aboveground biomass estimation
618 in amazonian tropical forests: a comparison of aircraft-and GatorEye UAV-borne LiDAR data in
619 the Chico Mendes Extractive Reserve in Acre, Brazil. Remote Sens. 12 (11), 1754.
620 https://doi.org/10.3390/rs12111754.

621 Drake, J.B., Dubayah, R.O., Clark, D.B. et al., 2002. Estimation of tropical forest structural
622 characteristics using large-footprint Lidar. Remote Sens. Environ. 79 (2-3), 305–319.
623 https://doi.org/10.1016/S0034-4257(01)00281-4.

624 Ellis, P.W., Griscom, B.W., Walker, W. et al., 2016. Mapping selective logging impacts in Borneo
625 with GPS and airborne Lidar. For. Ecol. Manag. 365, 184–196.
626 https://doi.org/10.1016/j.foreco.2016.01.020.

627 Espírito-Santo, F.D.B.; Gloor, M.; Keller, M.; et al., 2014. Size and frequency of natural forest
628 disturbances and the Amazon forest carbon balance. Nature communications 5, article number
629 3434. https://10.1038/ncomms4434.

630 ESRI, 2019. ArcMap software, ArcGIS Release 10.4. ESRI, Redlands, CA.

631 Farr, T.G., Rosen, P.A., Caro, E. et al., 2007. The shuttle radar topography mission. Rev.
632 Geophys. 45, RG2004. https://doi.org/10.1029/2005RG000183.

633 Ferraz, A., Saatchi, S., Mallet, C. et al., 2016. Lidar detection of individual tree size in tropical
634 forests. Remote Sens. Environ. 183, 318–333. https://doi.org/10.1016/j.rse.2016.05.028.

635 Figueiredo, E.O., Braz, E.M., d'Oliveira, M.V.N., 2007. Manejo de precisão em florestas tropicais:
636 modelo digital de exploração florestal. Embrapa Acre, Rio Branco.

637 Figueiredo, E.O., d'Oliveira, M.V.N., Braz, E.M. et al., 2016. Lidar-based estimation of bole
638 biomass for precision management of an Amazonian forest: comparisons of ground-based and
639 remotely sensed estimates. Remote Sens. Environ. 187, 281-293.
640 https://doi.org/10.1016/j.rse.2016.10.026.

641 Fox, J., Monette, J., 1992. Generalized collinearity diagnostics. J. Am. Stat. Assoc. 87 (417), 178-
642 183. https://doi.org/10.2307/2290467.

643 FUNTAC, 1990. Estrutura do plano de manejo de uso múltiplo da Floresta Estadual do Antimari.
644 Fundação de Tecnologia do Estado do Acre, Rio Branco.

645 González-Jaramillo, V., Fries, A., Bendix, J., 2019. AGB estimation in a tropical mountain forest
646 (TMF) by means of RGB and multispectral images using an unmanned aerial vehicle (UAV).
647 Remote Sens. 11 (12), 1413. https://doi.org/10.3390/rs11121413.

648 Griscom, B.W., Ellis, P.W., Burivalova, Z. et al., 2019. Reduced-impact logging in Borneo to
649 minimize carbon emissions and impacts on sensitive habitats while maintaining timber yields.
650 For. Ecol. Manag. 438, 176-185. https://doi.org/10.1016/j.foreco.2019.02.025.

651 Holmes, T.P.; Blate, G.M.; Zweed, J.C.; et al., 2002. Financial and ecological indicators of reduced
652 impact logging performance in the eastern Amazon. Forest Ecology and Management, 163: 93-
653 110. https://doi.org/10.1016/S0378-1127(01)00530-8.

654 Huang, W., Sun, G., Dubayah, R. et al., 2013. Mapping biomass change after forest disturbance:
655 applying LiDAR footprint-derived models at key map scales. Remote Sens. Environ. 134, 319–
656 332. https://doi.org/10.1016/j.rse.2013.03.017

657 Jarron, L.R., Coops, N.C., MacKenzieb, W.H. et al., 2020. Detection of sub-canopy forest structure
658 using airborne LiDAR. Remote Sens. Environ. 244, 111770.
659 https://doi.org/10.1016/j.rse.2020.111770.

660 Jayathunga, S., Owarib, T., Tsuyukia, S., 2018. The use of fixed–wing UAV photogrammetry with
661 LiDAR DTM to estimate merchantable volume and carbon stock in living biomass over a mixed
662 conifer–broadleaf forest. Int. J. Appl. Earth Obs. Geoinf. 73, 767–777.
663 https://doi.org/10.1016/j.jag.2018.08.017.

664 Jayathunga, S., Owari, T., Tsuyuki, S., 2019. Digital aerial photogrammetry for uneven-aged
665 forest management: assessing the potential to reconstruct canopy structure and estimate living
666 biomass. Remote Sens. 11 (3), 338. https://doi.org/10.3390/rs11030338.

667 Jensen, J.L.R., Mathews, A.J., 2016. Assessment of image-based point cloud products to generate
668 a bare earth surface and estimate canopy heights in a woodland ecosystem. Remote Sens. 8 (1),
669 50. https://doi.org/10.3390/rs8010050.

670 Kent, R., Lindsell, J.A., Laurin, G.V. et al., 2015. Airborne LiDAR detects selectively logged tropical
671 forest even in an advanced stage of recovery. Remote Sens. 7 (7), 8348-8367.
672 https://doi.org/10.3390/rs70708348.

673 Kronseder, K., Ballhorn, U., Böhm, V. et al., 2012. Above ground biomass estimation across forest
674 types at different degradation levels in Central Kalimantan using LiDAR data. Int. J. Appl. Earth
675 Obs. Geoinf. 18, 37–48. https://doi.org/10.1016/j.jag.2012.01.010.

676 Liu, Q., 2013. Integrating multi-source imagery data in a GIS system. International Archives of
677 the Photogrammetry, Remote Sensing and Spatial Information Sciences, Volume XL-7/W1, 3rd
678 ISPRS IWIDF 2013, 20 – 22 August 2013, Antu, Jilin Province, PR China.

679 Locks, C.J., 2017. Aplicações da tecnologia LiDAR no monitoramento da exploração madeireira
680 em áreas de concessão florestal. M.Sc. thesis, Universidade de Brasília, Brasília.

681 Longo, M., Keller, M.M., Dos-Santos, M.N. et al., 2016. Aboveground biomass variability across
682 intact and degraded forests in the Brazilian Amazon. Global Biogeochem. Cycles 30 (11), 1639-
683 1660. https://doi.org/10.1002/2016GB005465.

684 Lowe, D.G., 2004. Distinctive image features from scale-invariant key points. Int. J. Comput. Vis.
685 60 (2), 91-110. https://doi.org/10.1023/B:VISI.0000029664.99615.94.

686 Macpherson, A.J.; Schulze, M.D.; Carter, D.R.; Vidal, E., 2010. A Model for comparing reduced
687 impact logging with conventional logging for an Eastern Amazonian Forest. Forest Ecology and
688 Management 260: 2002-2011. doi:10.1016/j.foreco.2010.08.050

689 McDowell, N.; Allen, C.D.; Teixeira, K.A.; et al., 2018. Drivers and mechanisms of tree mortality
690 in moist tropical forests. New Phytologist, 219: 851-869. https://doi.org/10.1111/nph.15027

691 McGaughey, R.J., 2018. FUSION/LDV: software for LIDAR data analysis and visualization. United
692 States Department of Agriculture, Forest Service, Pacific Northwest Research Station,
693 Washington, DC.

694 Melendy, L., Hagen, S.C., Sullivan, F.B. et al., 2018. Automated method for measuring the extent
695 of selective logging damage with airborne LiDAR data. ISPRS J. Photogramm. Remote Sens. 139,
696 228–240. https://doi.org/10.1016/j.isprsjprs.2018.02.022.

697 Melo, A.W.F. de., 2017. Alometria de árvores e biomassa florestal na Amazônia Sul-Ocidental.
698 PhD Thesis, Instituto Nacional de Pesquisas da Amazônia.

699 Mendes de Moura, Y., Balzter, H., Galvão, L.S. et al., 2020. Carbon dynamics in a human-modified
700 tropical forest: a case study using multi-temporal LiDAR data. Remote Sens. 12 (3), 430.
701 https://doi.org/10.3390/rs12030430.

702 Meyer, V., Saatchi, S., Clark, D.B. et al., 2018. Canopy area of large trees explains aboveground
703 biomass variations across nine neotropical forest landscapes. Biogeosciences 15 (11), 3377-
704 3390. https://doi.org/10.5194/bg-15-3377-2018.

Ni, W., Dong, J., Sun, G. et al., 2019. Synthesis of leaf-on and leaf-of unmanned aerial vehicle (UAV) stereo Imagery for the inventory of aboveground biomass of deciduous forests. Remote Sens. 11 (7), 889. https://doi.org/10.3390/rs11070889.

Nunes, M.H., Jucker, T., Riutta, T. et al., 2021. Recovery of logged forest fragments in a human-modified tropical landscape during the 2015-16 El Niño. Nat. Commun. 12 (1), 1-11. https://doi.org/10.1038/s41467-020-20811-y.

Ota, T., Ogawa, M., Shimizu, K. et al., 2015. Aboveground biomass estimation using structure from motion approach with aerial photographs in a seasonal tropical forest. Forests 6 (11), 3882-3898. https://doi.org/10.3390/f6113882.

Ota, T., Ahmed, O.S., Minn, S.T. et al., 2019. Estimating selective logging impacts on aboveground biomass in tropical forests using digital aerial photography obtained before and after a logging event from an unmanned aerial vehicle. For. Ecol. Manag. 433, 162–169. https://doi.org/10.1016/j.foreco.2018.10.058.

Palace, M.W., Sullivan, F.B., Ducey, M.J. et al., 2015. Estimating forest structure in a tropical forest using field measurements, a synthetic model and discrete return lidar data. Remote Sens. of Environment 161, 1–11. https://doi.org/10.1016/j.rse.2015.01.020.

Pantoja, N.V., 2017. Alteração da cobertura florestal e biomassa em área de manejo florestal no Estado do Acre integrando dados de campo e sensores remotos. PhD Thesis, Instituto Nacional de Pesquisas da Amazônia.

Pereira, R.; Zweede, J.; Asner, G.P.; Kellerc, M., 2002. Forest canopy damage and recovery in reduced-impact and conventional selective logging in eastern Para, Brazil. Forest Ecology and Management 168 (2002) 77–89.

Phua, M., Hue, S.W., Ioki, K. et al., 2016. Estimating logged-over lowland rainforest aboveground biomass in Sabah, Malaysia using airborne LiDAR data. Terr. Atmos. Ocean. Sci. 27 (4), 481-489. 10.3319/TAO.2016.01.06.02(ISRS).

Pierzchała, M.; Talbot, B.; Astrup, R., Estimating Soil Displacement from Timber Extraction Trails in Steep Terrain: Application of an Unmanned Aircraft for 3D Modelling. Forests 2014, 5, 1212-1223; doi:10.3390/f5061212

Pinagé, E.R., Keller, M., Duffy, P. et al., 2019. Long-term impacts of selective logging on Amazon forest dynamics from multi-temporal airborne LiDAR. Remote Sens. 11 (6), 709. https://doi.org/10.3390/rs11060709.

Prandi, F., Magliocchetti, D., Poveda, A. et al., 2016. New approach for forest inventory estimation and timber harvesting planning in mountain areas: The SLOPE Project. Int. Arch. Photogramm. Remote Sens. Spatial Inf. Sci. XLI-B3, 775-201. https://doi.org/10.5194/isprs-archives-XLI-B3-775-2016.

Prata, G. A., Broadbent, E. N., de Almeida, et al., 2020. Single-Pass UAV-Borne GatorEye LiDAR Sampling as a Rapid Assessment Method for Surveying Forest Structure. Remote Sensing, 12(24), 4111.

Putz, F.E.; Sist, P.; Fredericksen, T.; Dykstra, D., 2008. Reduced-impact logging: Challenges and opportunities. Forest Ecology and Management 256: 1427-1433

745 Réjou-Méchain, M., Tymen, B., Blanc, L. et al., 2015. Using repeated small-footprint LiDAR
746 acquisitions to infer spatial and temporal variations of a high-biomass Neotropical forest.
747 Remote Sens. Environ. 169, 93–101. https://doi.org/10.1016/j.rse.2015.08.001

748 Rex, F.E., Silva, C.A., Dalla Corte, A.P. et al., 2020. Comparison of statistical modelling approaches
749 for estimating tropical forest aboveground biomass stock and reporting their changes in low-
750 intensity logging areas using multi-temporal LiDAR data. Remote Sens. 12 (9), 1498.
751 https://doi.org/10.3390/rs12091498.

752 Saatchi, S., Xu, A., Meyer, V. et al., 2017. Carbon map of DRC: a summary report of UCLA Institute
753 of Environment &Sustainability. UCLA, Los Angeles.

754 Salach, A., Bakuła, K., Pilarska, M. et al., 2018. Accuracy assessment of point clouds from LiDAR
755 and dense image matching acquired using the UAV Platform for DTM Creation. *ISPRS Int. J. Geo-*
756 *Inf.* 7 (9), 342. https://doi.org/10.3390/ijgi7090342.

757 Silva, C.A., Hudak, A.T., Vierling, L.A. et al., 2017. Impacts of airborne Lidar pulse density on
758 estimating biomass stocks and changes in a selectively logged tropical forest. Remote Sens. 9
759 (10), 1068. https://doi.org/10.3390/rs9101068.

760 Sist, P. Ferreira, F.N., 2007. Sustainability of reduced-impact logging in the Eastern Amazon.
761 Forest Ecology and Management, 243: 119-209. https://doi.org/10.1016/j.foreco.2007.02.014

762 Stark, S.C., Breshears, D.D., Aragón, S., et al., 2020. Reframing tropical savannization: linking
763 changes in canopy structure to energy balance alterations that impact climate. Ecosphere 11
764 (9), e03231. https://doi.org/10.1002/ecs2.3231.

765 Swinfield, T., Lindsell, J.A., Williams, J.V. et al., 2019. Accurate measurement of tropical forest
766 canopy heights and aboveground carbon using structure from motion. Remote Sens. 11 (8), 928.
767 https://doi.org/10.3390/rs11080928.

768 Van Leeuwen, M., Nieuwenhuis, M., 2010 Retrieval of forest structural parameters using LiDAR
769 remote sensing. Eur. J. For. Res. 129, 749–770. https://doi.org/10.1007/s10342-010-0381-4.

770 Valbuena, R; O'Connor, B.; Zellweger, F.,2020. Standardizing Ecosystem Morphological Traits
771 from 3D Information Sources. Trends in Ecology & Evolution,
772 https://doi.org/10.1016/j.tree.2020.03.006.

773 Wallace, L., Lucieer, A., Malenovský, Z. et al., 2016. Assessment of forest structure using two
774 UAV techniques: a comparison of airborne laser scanning and structure from motion (SfM) point
775 clouds. Forests 7 (3), 62. https://doi.org/10.3390/f7030062.

776 White, J.C., Wulder, M.A., Vastaranta, M. et al., 2013. The Utility of image-based point clouds
777 for forest inventory: a comparison with airborne laser scanning. Forests 4 (3), 518-536.
778 https://doi.org/10.3390/f4030518.

779 Wulder, M.A., Bater, C.W., Coops, N.C. et al., 2008. The Role of LiDAR in sustainable forest
780 management. For. Chron. 84 (6), 807-826. https://doi.org/10.5558/tfc84807-6.

781 Zahawi, R.A.; Dandois, J.P.; Holl, K.D.; Nadwodny, D.; Reid, J.L.; Ellis, E.C., 2015. Using lightweight
782 unmanned aerial vehicles to monitor tropical forest recovery. Biological Conservation 186 (2015)
783 287–295.

784 Zimmerman, B.L. & Kormos, C.F, 2012. Prospects for Sustainable Logging in Tropical Forests.
785 BioScience 62: 479–487. doi:10.1525/bio.2012.62.5.9.

786 Zhao, X., Su, Y., Hu, T. et al., 2018. A global corrected SRTM DEM product for vegetated areas.
787 Remote Sens. Lett. 9 (4), 393-402. https://doi.org/10.1080/2150704X.2018.1425560.

788